

# Using Simulated 3D Surface Fuelbeds and Terrestrial Laser Scan Data to Develop Inputs to Fire Behavior Models

Eric Rowell, E. Louise Loudermilk, Carl Seielstad & Joseph J. O'Brien

To cite this article: Eric Rowell, E. Louise Loudermilk, Carl Seielstad & Joseph J. O'Brien (2016): Using Simulated 3D Surface Fuelbeds and Terrestrial Laser Scan Data to Develop Inputs to Fire Behavior Models, Canadian Journal of Remote Sensing, DOI: [10.1080/07038992.2016.1220827](https://doi.org/10.1080/07038992.2016.1220827)

To link to this article: <http://dx.doi.org/10.1080/07038992.2016.1220827>



Accepted author version posted online: 05 Aug 2016.  
Published online: 05 Aug 2016.



Submit your article to this journal [↗](#)



Article views: 21



View related articles [↗](#)



View Crossmark data [↗](#)

# Using Simulated 3D Surface Fuelbeds and Terrestrial Laser Scan Data to Develop Inputs to Fire Behavior Models

Eric Rowell<sup>1,\*</sup>, E. Louise Loudermilk<sup>2</sup>, Carl Seielstad<sup>3</sup>,  
and Joseph J. O'Brien<sup>2</sup>

<sup>1</sup>National Center for Landscape Fire Analysis, The University of Montana, 32 Campus Drive, Missoula, MT 59812, USA

<sup>2</sup>USDA Forest Service, Southern Research Station, Center for Forest Disturbance Science, 320 Green Street, Athens, GA 30602, USA

<sup>3</sup>Department of Forest Management, College of Forestry and Conservation, The University of Montana, 32 Campus Drive, Missoula, MT 59812, USA

**Abstract.** Understanding fine-scale variability in understory fuels is increasingly important as physics-based fire behavior models drive needs for higher-resolution data. Describing fuelbeds 3Dly is critical in determining vertical and horizontal distributions of fuel elements and the mass, especially in frequently burned pine ecosystems where fine-scale fuels arrangement drives fire intensity and resulting fire effects. Here, we describe research involving the use of highly resolved 3D models. We create fuelbeds using individual grass, litter, and pinecone models designed from field measurements. These fuel models are distributed throughout the fuelbed to replicate fuel distribution in rectified nadir photography taken for each plot. The simulated fuelbeds are converted into voxel arrays and biomass is estimated from calculated surface area between mesh vertices for each voxel. We compare field-based fuel depth and biomass with simulated estimates to demonstrate similarities and differences. Biomass distributions between simulated fuel beds and terrestrial laser scan data correlated well using Weibull shape parameters ( $r = 0.86$ ). Our findings indicate that integration of field, simulated, and terrestrial laser scanner data will improve characterization of fuel mass, type, and spatial allocations that are important inputs to physics-based fire behavior models.

**Résumé.** La compréhension de la variabilité à petite échelle du sous-bois combustible est de plus en plus importante étant donné que les modèles de comportement du feu basés sur la physique motivent le besoin d'avoir des données de plus haute résolution. La description des couches de combustibles en 3 dimensions est essentielle pour déterminer les distributions verticales et horizontales des éléments combustibles et la masse, en particulier dans les écosystèmes de pin fréquemment brûlés, où la structure des combustibles à fine échelle détermine l'intensité du feu et les effets résultants du feu. Nous décrivons ici une étude impliquant l'utilisation des modèles en 3 dimensions à haute résolution. Nous créons des couches de combustible utilisant des modèles individuels de l'herbe, de la litière et des pommes de pin conçus à partir de mesures sur le terrain. Ces modèles de combustible sont distribués dans toute la couche de combustible pour reproduire la distribution des combustibles dans l'imagerie au nadir rectifiée prise pour chaque parcelle. Les couches de combustible simulées sont converties en tableaux de voxels et la biomasse est estimée à partir de la surface calculée entre les sommets du maillage pour chaque voxel. Nous comparons la profondeur et la biomasse de combustible sur le terrain avec des estimations simulées pour démontrer les similarités et les différences. Les distributions de la biomasse entre les couches de combustible simulées et les données de balayage laser terrestre étaient bien corrélées en utilisant des paramètres de forme de Weibull ( $r = 0,86$ ). Nos résultats indiquent que l'intégration des données de terrain, simulées et provenant du balayage laser terrestre permettra d'améliorer la caractérisation de la masse, du type et des distributions spatiales de combustible qui sont des intrants importants pour les modèles de comportement du feu basés sur la physique.

## INTRODUCTION

The ability to spatially describe wildland fuels across an array of scales is critical for decision making in operational wildfire and prescribed fire management (Mutch et al. 1993; Keane et al.

2001). Spatial fuels data have historically been used in fuels planning, fire behavior and effects modeling, and hazard assessment. With recent advances in fire behavior modeling, the need for these types of data has expanded to include higher-resolution 3D characteristics. New complex fluid dynamics models provide opportunities to examine the fine spatial scale ( $< 1$  m) of fire behavior, which potentially drives larger-scale fire behavior and might spatially organize ecosystems (Hiers et al. 2009). These

Received 19 October 2015. Accepted 24 July 2016.

\*Corresponding author e-mail: eric.rowell@firecenter.umt.edu.

models rely on appropriately dimensioned fuels data, which are not readily available from conventional sampling techniques. The basis for fuels measurements has been to provide a generalized fuels description, while considering that collecting all physical attributes of a fuel bed is usually intractable (Keane et al. 2001). In 2001, the Core Fire Science Caucus, a self-directed group of fire scientists, elucidated the need for a new context within which to describe fuels that coupled with advances in fire behavior and smoke modeling (Sandberg et al. 2003; Hardy et al. 2008). Fuel measurement methods were developed to support coarse-grained fire behavior or fire effects modeling that do not encompass the full range of heterogeneity or spatial nonuniformity in fuels found within and across landscapes (Hardy et al. 2008). Similar limitations are noted in the realm of ecology, where conventional methods of inventory are designed to classify abundance of dominant vegetation rather than individual organisms using most common species characterization (Thompson 2004).

Fire is a dynamic process, influenced by discontinuities and variabilities that are not fully captured in traditional fuels measurements. Commonly used direct measurements of fuels are taken from planar transects or point intercept coupled with dry-weighed biomass samples (Brown 1974; Brown 1981). These direct sample protocols are labor intensive and limited in scale and they are not efficient at estimating fine fuels such as grasses (Loudermilk et al. 2009). Estimation of bulk density of shrubs and grasses requires unrealistic assumptions that inherently oversimplify the fuel elements (Van Wagner 1968). Yet, fine-scale patterns of surface fuels are complex and relate to spatial measurements of fire intensity in low-intensity fire regimes (Loudermilk et al. 2012; Loudermilk et al. 2014). Fine-scale fire effects have also been commonly described in frequently burned pine conifer forests, where variability of fire intensity depends on the matrix and orientation of flammable grasses, forbs, shrubs, and pine needles (Thaxton and Platt 2006, Mitchell et al. 2009). New fire behavior models combined with new fuels measurement techniques are now providing opportunities to better understand patterns of fuels and the effects of fine-scale fire behavior, and the research community is active in rethinking approaches to fuels inventory and developing alternative methods (Hiers et al. 2009).

A relatively new approach to characterize fuels is by application of active remote sensing in the form of Light Detection and Ranging (LiDAR), which potentially characterizes fuelbeds continuously by collecting height and reflectance properties of fuel objects (Seielstad and Queen 2003; Hudak et al. 2016). LiDAR remote sensing is limited in its ability to directly match biophysical parameters with similar field measurements (Popescu et al. 2002; Hopkinson et al. 2005; Riaño et al. 2007; Strecker and Glenn 2006; Glenn et al. 2010). Platforms such as terrestrial laser scanners (TLS) collect enormous quantities of point data (mm to cm point spacing) for small areas (1 m–1 ha), but are victim to issues of sampling variability. TLS point density degrades over distance, and data collection must be executed

from multiple angles in order to reduce the effects of occlusion as energy is intercepted by taller and larger objects that shadow the other parts of the scan (Hosoi and Omasa 2006; Rowell et al. 2015). Moreover, studies are generally limited to extraction of biometrics of individual identifiable objects within larger fuelbeds, for example, for shrubs in open arctic environments (Vierling et al. 2013; Greaves et al. 2015) and sagebrush steppe (Olsoy et al. 2014). Attempts at characterizing mixed fuelbeds (e.g., nearly all fuelbeds at fine grain) with TLS have shown the difficulties in unmixing objects or types within laser point clouds to characterize mass and heights per fuel type (Loudermilk et al. 2009; Rowell and Seielstad 2012; Rowell et al. 2015).

To address limitations of TLS, one approach uses parametric plant models to simulate biomass distributions. A small number of studies are utilizing 3D models of trees and plants to produce object-based simulations of ecosystems for use in a variety of applications, such as simulations to assess spectral properties of plants (Disney et al. 2009; Cawse-Nicholson et al. 2013; Woodgate et al. 2015) and modeling of airborne LiDAR data for individual tree inspection in forested environments (Disney et al. 2010; Disney et al. 2011). A related method for individual plant modeling is the application of the Lindenmayer system (L-systems) fractal modeling for virtual construction of xeric shrubs for use in leaf-scale fire behavior simulations (Prince 2014, Prince et al. 2014). L-systems used in Prince et al. (2014) grow fractal plant features using assigned angles of rotation representative of the specific plant morphology. Prince et al. (2014) showed that bulk densities similar to those reported in the literature could be obtained from geometrically correct plant models of chamise, manzanita, and Utah juniper. In similar work, Parsons et al. (2011) used probability functions to distribute biomass throughout individual tree canopies as a collection of simple shapes (cylinders and frustrums), using a pipe model approach. This approach has yielded highly detailed tree models that are applied in the FUEL3D model for improved understanding of fire dynamics within forest stands. FUEL3D uses allometric estimates of biomass based on inputs from the Forest Vegetation Simulator<sup>1</sup> that are distributed throughout individual trees as partitions of bole, branch, and needles. All of these studies focus on modeling the individual tree and shrub canopies. As of this study, there has been no similar examination of understory vegetation and surface fuels focused on construction of 3D assemblages of mixed fuel elements.

Here, we present methods for constructing spatially explicit, highly resolved, and realistic fuelbeds using tools developed for 3D animation and modeling. Each fuel element/type (e.g., shrub, grass, needle, etc.) is discretized in the fuelbed, allowing for direct accounting of metrics such as height, volume, cover, surface area, density, and mass. We then examine the fuelbeds

<sup>1</sup>FVS, United States Forest Service, <http://www.fs.fed.us/fmcs/fvs/>

through comparison with in situ nadir imagery and field measurements and explore the utility of these models as tools to better understand spatial variability in fuel properties and to improve remote sensing of fuelbeds and fine-grained fire modeling. Finally, we compare simulated fuelbed height distributions with TLS-derived height distributions to assess correspondence of the 2 methods as a preamble to future incorporation of LiDAR ray-tracing for simulating TLS.

Our research centers on a main objective of developing realistic and quantifiable simulated surface fuelbeds in longleaf pine ecosystems. We approached this objective in 3 phases: (i) we generated fuel simulations from parametric plant models using high resolution nadir photo imagery and detailed height measurements and parameterized them with biomass estimates for discrete fuel elements; (ii) we transposed the models to an independent validation site and compared biomass estimates to actual dry weights; and (iii) we derived and contrasted height distributions from the simulations and TLS data.

## METHODS

### Study Area

Two field campaigns were conducted to acquire data at Eglin Air Force Base (AFB), Florida, in October 2012 and February 2014. Eglin AFB (30° 32' 12" N, 86° 43' 44" W) is located in the panhandle of northwestern Florida, in the United States, which was originally a unit of the former Choctawhatchee National Forest; Eglin is an important resource in the management of longleaf pine ecosystems, with 180,000 ha of longleaf pine sandhills and flatwoods.

### Field Observations

The October 2012 data were collected as part of the Prescribed Fire Combustion and Atmospheric Dynamics Research Experiment (RxCadre) funded by the Joint Fire Sciences Program (11-2-1-11). Fuels data were collected at 23 0.5 m<sup>2</sup> plots around small replicate prescribed fire sampling blocks (20 m x 20 m) nested within a larger burn unit. These small replicate blocks are referred to as highly instrumented plots (HIPs). Height metrics for each plot were collected (maximum and mean height for grass, forbs, shrubs, and litter). Each plot was clipped of all vegetation, sorted by fuel type, and samples were oven dried at 70 °C for 48 hours and then weighed (Ottmar et al. 2016).

The February 2014 data were collected as part of a Department of Defense Strategic Environmental Research and Development Program (SERDP) funded project (#RC-2243). Vegetation and fuel characteristics were gathered in 99 plots located in longleaf pine sandhills of Eglin AFB. Plots measured 1 m x 3 m in size and were gridded into cells measuring 10 cm by 10 cm, so that each of the 9 plots contained 300 cells. For each

cell, point intercept measurements of plant species and fuelbed height were collected. Fuel measurements included fuel and litter depths (cm), and presence or absence of fuels. As part of a separate experiment (O'Brien et al., in review), longleaf cones were randomly distributed at densities of 0 per m<sup>2</sup>, 5 per m<sup>2</sup>, or 10 per m<sup>2</sup>.

### Workflow Description

Workflow is divided into 3 phases (Figure 1).

Phase 1: model development and parameterization,  
Phase 2: replication and validation of simulations, and  
Phase 3: TLS and simulation comparison.

Phase 1 outlines the development of plant models and construction of fuelbeds via interpretation of nadir and oblique photography and subsequent application of generalized fuel mass allocations. Phase 1 outlines the development of these methods and application of generalized fuel mass allocations (see surface area and fuel mass). Phase 2 describes the replication of the technique at an independent site along with comparisons of simulated and measured biomass and height. Phase 3 examines the derivation and comparison of TLS-based and simulated height distributions.

### Fuelbed Simulations

Simulated fuelbeds (Figure 2) were generated through a series of steps starting with the Onyx Garden Suite,<sup>2</sup> a parametric plant modeling system that allows users to adjust physical parameters of individual plant elements to create 3D plant models. This model generator was used to produce individual plant elements representative of types observed in our field plots. Fuel elements for each plant model were selected based on primary life-form measurements collected in the field campaign, including models of tall grass (senesced), moderate stature grass (senesced), low grass (senesced), tall shrubs, low shrubs (senesced), low shrubs (evergreen), longleaf pine litter, deciduous oak litter, other deciduous litter, and longleaf pine cones. Height dimensions of the models were parameterized based on average heights coincident with identifiable plants located in nadir photographs collected at each plot. The horizontal extent of plant elements and objects in the litter were determined from measurements in rectified plot photos in a Cartesian coordinate space, using the southwest corner of the plot as the origin.

Fuelbeds were constructed as assemblages of plants, litter, and cones using the freeware Blender 2.74.<sup>3</sup> Blender is typically used as a platform to produce scenes and objects for 3D

<sup>2</sup>Onyx Computing Inc. 1992-2008, <http://www.onyxtree.com>

<sup>3</sup>[www.blender.org](http://www.blender.org)

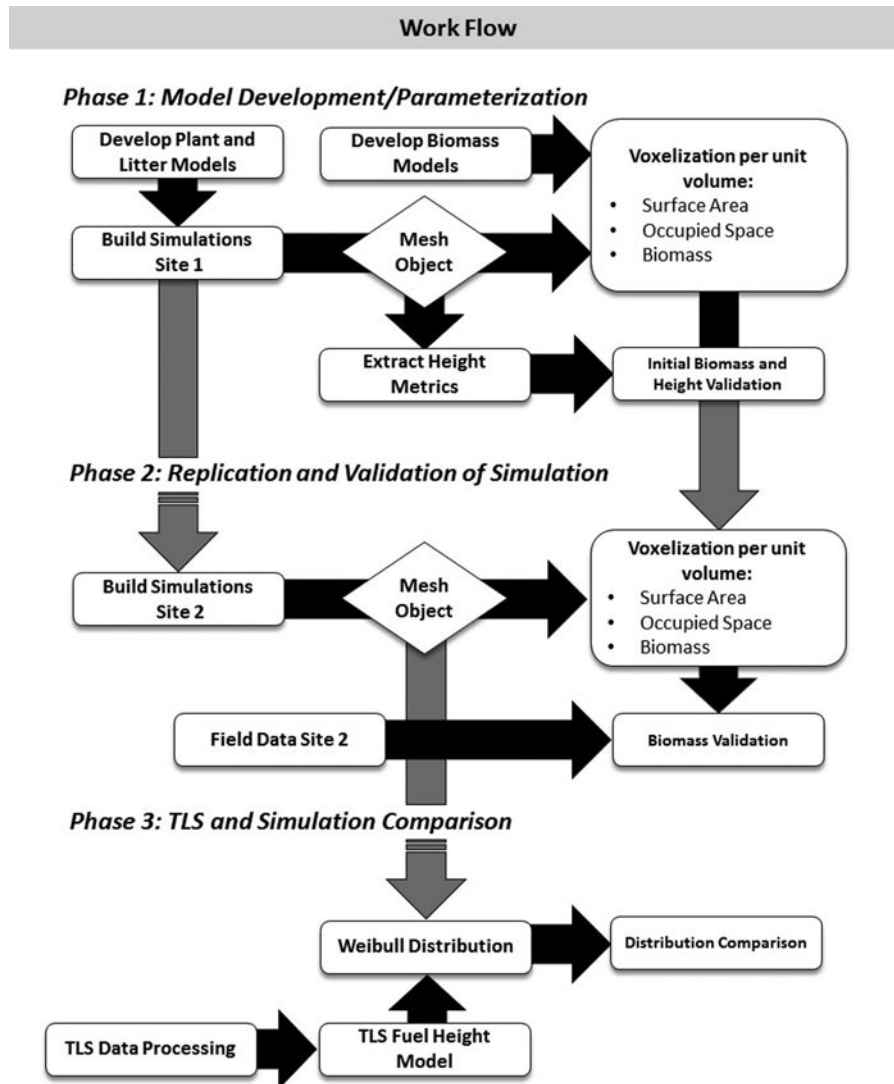


FIG. 1. The diagram depicts the 3 phases of work conducted to (Phase 1) produce fuel simulations, (Phase 2) replicate and validate biomass at an independent site, and (Phase 3) compare simulated and TLS height distributions.

renderings for use in graphic design and tree-dimensional animation applications. Onyx-based plant and litter objects were imported into the Blender environment as wavefront open format file input (.obj). Identifiable objects such as tall grass, isolated moderate stature grass, shrubs, and cones, were positioned by their Cartesian coordinates as measured in the rectified high-resolution nadir plot photography in the ArcGIS environment.<sup>4</sup> Each fuel element contains an anchor point representing the center of the object on the ground plane. This point was the location used to place each element. Distributions of other fuel elements such as clusters of deciduous litter, long-leaf litter, and congruous clumps of grass were placed within bounded areas as

defined by presence/absence of each fuel type specified by the field-collected point intercept data. Groupings of fuel elements were refined based on visual comparison with plot photography, because the point intercept data omits areas of data between sample points. The final scenes were exported to an x,y,z text format representing the fuel bed with all elements included (e.g., herbaceous plants and grasses, needles, oak leaves, litter, and cones). Each x,y,z point represents a vertex from a mesh object of a fuel element and is attributed with a specific fuel type (e.g., grass, needle, cone, etc.)

The SERDP data were used to develop and parametrize the models in Phase 1 as the spatial resolution of the nadir photo imagery and density of measured fuelbed heights were more highly resolved than in the data collected from the RxCadre experiment. The simulation techniques developed from the SERDP project

<sup>4</sup>Environmental Research Systems Institute, Redlands, California, USA

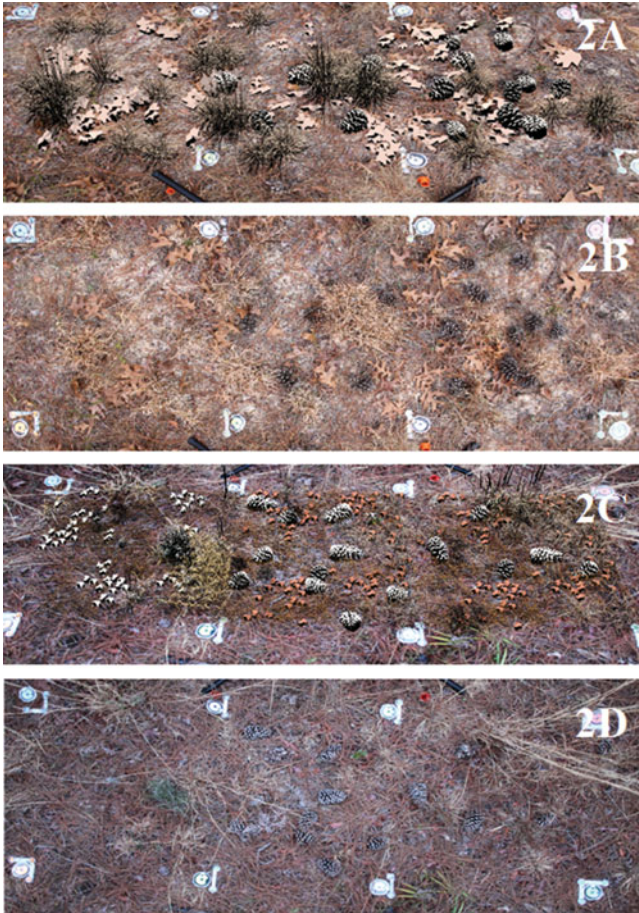


FIG. 2. A comparison of synthetic fuelbeds for (2A) plot 1 with (2B) the nadir plot photo and (2C) plot 7 synthetic fuelbed with (2D) the nadir plot photo. This comparison demonstrates that placement of objects is coincident between photo and the synthetic fuelbed, and the objects used to populate that simulation behave like real plants, with some generalization.

were replicated for the RxCadre data. However, because these data were less intensively sampled for fuelbed height metrics (Figure 3), oblique imagery was used to place fuel elements in the simulation.

### Voxelization

A voxelized approach was taken to reduce the dimensionality of the data and to exploit analysis techniques that rely on cell-based arrays. Each fuelbed was voxelized, using the approach outlined in Hosoi and Omasa (2006). Voxels, 3D pixels that allow for volumetric representation of discontinuous surfaces by using a regularly spaced 3D grid, were developed (Stoker 2009). A 3D search cube was applied to the  $x,y,z$  files to summarize the number of fuel vertices found within each  $1\text{ cm}^3$ . A benefit of voxel analysis is the ability to depict areas of missing and present data in geometric space. In the domain of fuelbed geometry, voxelization allows for the ability to examine connectivity in

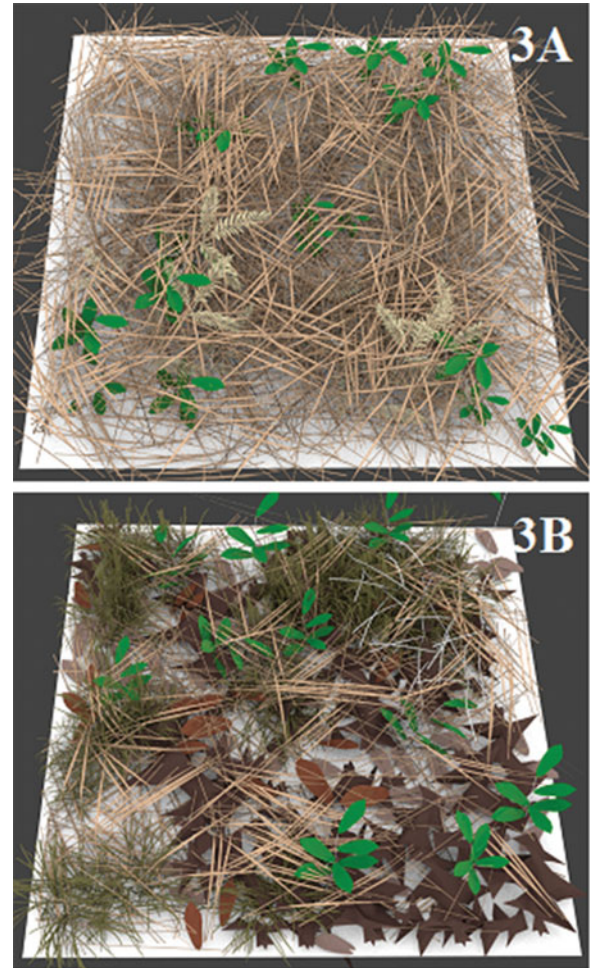


FIG. 3. A comparison of synthetic fuelbeds generated for the RxCadre plots representing (3A) longleaf pine litter and forb fuel matrix and (3B) mixed longleaf pine and turkey oak litter with a grass and forb overstory fuelbed. These depictions represent examples of how fuels vary in distribution type and arrangement within the site at Eglin AFB, Florida, USA.

3 dimensions, which is paramount to understanding where fuel elements exist and how they are distributed in space. The  $1\text{ cm}^3$  voxel resolution was selected based on 2 criteria:

- (i) Within the shrub grassland matrix  $1\text{ cm}^3$  voxel cells allow for characterization of both clusters of grass clumps (grass blades are typically  $\leq 1\text{ cm}$  in width) and larger shrub components (e.g., leaves and branches  $> 1\text{ cm}$  in width).
- (ii) This grain size preserves gaps between clusters of fuel elements. Larger grains (e.g.,  $>$  decimeter) begin to fill gaps and generalize the fuelbed in ways that limit further analysis.

### Filled Volume

Previous work using TLS of grass-shrub fuelbeds has shown that plant material concentrates in the lower part of the fuelbed in

the form of densely clustered leaves and stems of grass bunches and plant litter, and the upper part of the fuelbeds typically contain more dispersed stems and grass inflorescence (Rowell and Seielstad 2012; Rowell et al. 2015). Total occupied volume of each 1-m<sup>2</sup> subplot was calculated by summing the total number of occupied voxel cells present.

### Surface Area and Fuel Mass

To realize the full value of modeled fuelbeds for examining fuels variability, it was necessary to relate the vertices that define each fuel element to specific fuel properties. Vertices density was determined to be a poor representation of plant material, because some plants that have large amounts of biomass were represented by a relatively small numbers of vertices in the plant models. To overcome this, we calculated fuel surface area for each fuel type, using the MESH\_SURFACEAREA routine in IDL<sup>5</sup> for each 1 cm<sup>3</sup> voxel cell in. The meshing algorithm used incorporates mesh normals to connect vertices, allowing calculation of the surface area for each resulting polygon. Total surface areas per 1-m<sup>2</sup> subplot are reported in Table 3. We then used the surface area calculations to weight mass per occupied volume in our simulated fuelbeds on a voxel-by-voxel basis. Additional information concerning fuel mass and fuel volume are needed to impute bulk density, particle density, and packing ratio. For fuel mass, we examined the literature to find general data describing fine-grained biomass properties of representative grasses, longleaf pine litter and cones, and turkey oak leaves (Table 1). We used the shrub biomass properties for the forb biomass estimation because we were unable to find appropriate biomass estimates for this fuel type. Then, we calculated an average mass of each fuel (derived from the literature using values described in Brockway and Outcalt 2000; Fonda and Varner 2004; Fonda 2001; and Kane et al. 2008) per mm<sup>2</sup>. For example, for grass we took the average mass-per-unit area reported in the literature for the species little bluestem and used associated cover and height to generate a plant volume. From these dimensions we calculated a mass per area (mm<sup>2</sup>) for each plant/litter model. For cones, we use average mass of a longleaf pine cone divided by average volume of cones in our dataset. These average density estimates were used to distribute biomass within each element in the simulated fuelbeds in the following way. The purpose of this admittedly indirect method of biomass estimation was to account for the high variability in vertex density within fuel elements that is not obviously related to density of biomass. The weighting assumes that surface area calculated from our meshes is directly related to mass.

### Calculating Height Metrics

Height metrics were extracted from the simulated fuelbeds on a 10-cm grid within each plot by applying a 10-cm equal-spaced point array and sampling a 10-cm<sup>2</sup> area around each centroid.

Height metrics were compared only within the SERDP data; the RxCadre data were collected as plot averages and were not spatially explicit. Fuel depth from the simulated fuelbed represents all heights found in the area opposed to the point intercept data collected in the field, which documents only intercepted heights at a point. Although we could have used the same approach and considered only those objects from the modeled fuelbed that fell on top of the field-measured points, it is extremely unlikely that field measurements would precisely coincide with features of our plant models, and we instead chose to include any point found within the search area so we could express height variability per fuel cell. By applying the point network from our point intercept data to the simulated fuelbeds, we also developed a suite of height metrics, including maximum, 99th percentile, mean, inflection height, standard deviation, median height, standard deviation height, kurtosis, and skewness. All heights within a 100-cm<sup>2</sup> area around each field sample point were used to calculate these metrics from the artificial fuelbeds at a grain of 10cm. These metrics were ultimately compared to coincident field-observed heights.

### Terrestrial Laser Scanning Collection and Processing

Laser scans were collected pre- and postfire using an Optech ILRIS<sup>TM</sup> 36D-HD laser scanner at a 10kHz sampling frequency. Data were collected for the L2 forested burn blocks (RxCadre), which contained 2 years of fuel accumulation and plant growth since the previous prescribed fire. The TLS instrument was positioned at the 4 corners of the HIPs plot, positioned an average distance of 7 m from the edge of the plot on a telescoping tripod set at a height of 2.74 m. The laser was pointed downward with an average inclination of  $-30^\circ$  and a focal range of 20 m, resulting in an average scan density of 8.4 mm. Reflective posts were placed on the southeast corner of every 0.25-m<sup>2</sup> sample plot around each HIPS plot, resulting in 12 tie points per HIPs.

TLSs were aligned using the Polyworks<sup>6</sup> software suite and further point cloud spatial refinements were completed using CloudCompare,<sup>7</sup> an open source point alignment software package. Individual scans were merged together into a single dataset and projected on a UTM coordinate system through coincident GPS data collected for all HIPs corner points. A more in-depth processing explanation can be found in Rowell et al. (2015). Point clouds were subset into individual sample plots ( $n = 23$ ) by locating the reflective post on each corner and defining a clip polygon feature in ArcGIS. A fuel height model (FHM) was generated by subtracting the geoid height from a local minimum height, producing normalized height above ground. TLS point clouds were imported into R<sup>8</sup> for statistical analysis.

<sup>6</sup>Innovmetric, Quebec, Canada

<sup>7</sup>CloudCompare 2014; [www.cloudcompare.org](http://www.cloudcompare.org)

<sup>8</sup>[www.r-project.org](http://www.r-project.org)

<sup>5</sup>Exelis VIS, Boulder, Colorado, USA

TABLE 1

List of the studies used to produce the portioned biomass allocation used to predict the biomass for each voxel for little blue stem, turkey oak litter, longleaf pine litter, and longleaf cones. Biomass partitions are reduced to biomass for grams per mm<sup>2</sup>.

Grasses								
Fuel Type	Study	Study site	Treatment	Reference Biomass	Reference Units	Cover (%)	Height (cm)	Biomass (grams/mm <sup>2</sup> )
<i>Aristida stricta</i> Michx.	Brockway et al. 1998	Marion County, FL	Herbicide	15.5	Grams per m <sup>2</sup>	57.8	*	0.00155
Cones								
Fuel Type	Study	Study site	Treatment	Reference Biomass	Reference Units	Cover (%)	Length (cm)	Biomass (grams/mm <sup>3</sup> )
<i>Pinus palustris</i>	Fonda and Varner 2004	Ocala, FL	—	59.1	Grams per cone	—	**	0.000591
Longleaf Pine Litter								
Fuel Type	Study	Study site	Treatment	Reference Biomass	Reference Units	Cover (%)	Height (cm)	Biomass (grams/mm <sup>2</sup> )
<i>Pinus palustris</i>	Fonda 2001	Ocala, FL	2x2 Factorial design	14.21	Grams per m <sup>2</sup>	100	5	0.002321
Turkey Oak Litter								
Fuel Type	Study	Study site	Treatment	Reference Biomass	Reference Units	Cover (%)	Height (cm)	Biomass (grams/mm <sup>2</sup> )
<i>Quercus Laevis</i>	Kane et al. 2008	Jones Ecological Center	Lab experiment	15	Grams per 35 cm <sup>2</sup>	100	6.2	0.000197

\*30 cm from the other studies was substituted for the height as there were no published heights associated with the Derner et al. 2012 or Brockway and Outcalt 2000 studies.

\*\*No dimensions of the cones are reported in Fonda and Varner 2004, so dimensions were measured from the nadir plot photos.

### Statistical Analysis

Analyses are presented in the 3 phases described previously; Phase 1: parameterization and development of simulated fuelbeds and biomass estimations using high resolution nadir imagery and field-based height data ( $n = 100$  data points per plot) for the SERDP site. Height comparison is conducted using the Pearson correlation. Phase 2: replication of model development and biomass estimation for the RxCadre site and comparison with in situ measurements of biomass. Comparisons are conducted using Pearson correlation, ANOVA, and RMSE. Phase 3: fuelbed height distributions comparison between TLS-based and simulation-based, using Weibull distribution functions to analyze shape ( $\alpha$ ) and scale ( $\beta$ ) parameters using the fitdistrplus package (Delignette-Muller and Dutang 2015) in R. The Weibull function is fit to the TLS and simulated fuel height

model using the maximum likelihood estimate method. We also used a regression-based equivalence test (Robinson et al. 2005) in the equivalence package in R (Robinson 2016) to test the intercept equality between 2 measurements. The region of equality was determined to be  $\pm 25\%$  of the mean for the intercept and slope. Rejection of the null hypothesis is where the interval of equivalence contains the 95% confidence interval, maintaining that there is no dissimilarity.

### RESULTS

#### Phase 1: Parametrization and Simulation Development in the SERDP Plots

The simulated fuelbeds closely resembled the plot photos in appearance and geometry (Figure 2) and share characteristics with field measurements in terms of fuel depth

TABLE 2

Simulated fuelbed heights correlate well with measured fuel depth, with most variability resulting from grass blades in the simulation crossing in the 10 cm<sup>2</sup> grid cell. Residual standard errors (RSE) were greatest in Plot 3, which had a lattice of reproductive grass stems that were bent across the plot

Plot	Correlation	df	p-value	Confidence Interval (95 %)	RSE
1	0.94	298	< 0.001	0.92–0.95	5.76
2	0.81	298	< 0.001	0.81–0.87	8.98
3	0.84	298	< 0.001	0.80–0.87	14.36
4	0.75	298	< 0.001	0.69–0.79	4.88
5	0.86	298	< 0.001	0.82–0.88	3.70
6	0.96	298	< 0.001	0.94–0.96	2.21
7	0.88	298	< 0.001	0.85–0.90	5.76

and cover. In this study, fuel depth and cover are the only directly comparable metrics between the field-measured and the simulated fuelbed data, because no other field data were collected.

### Height Metrics

Comparisons of field and simulated fuel depth (Table 2) were well correlated with correlation coefficients ranging from 0.75 to 0.96. The tightest correspondence occurred in plot 6 ( $r = 0.96$ ,  $p$ -value < 0.001). Plots with high densities of overhanging grass stems proved most variable when compared against the point intercept data with correlation coefficients ranging from 0.81 to 0.88. In all cases, the tallest measurements from the field and simulated fuel heights related well, with less correspondence in the lower reaches of the fuel beds. Plots with generally low stature fuels and isolated taller grass fuels performed best. The largest residual standard error occurred in plot 3, where a lattice of overhanging grass stems crisscrossed the plot. The field point intercept data often miss these sparse objects, whereas careful attention was given to adding them in generation of the simulated fuelbeds.

### Biomass Estimation

Estimates of per-subplot biomass fell within expected ranges reported in the literature (Table 3) for grass, needles, cones, and deciduous litter, with 3 exceptions. Ranges for grass biomass were from 43.43 grams/m<sup>2</sup> to 664.22 grams/m<sup>2</sup>, needle litter ranged from 0.23 grams/m<sup>2</sup> to 35.23 grams/m<sup>2</sup>, and cone biomass ranged from 117.96 grams/m<sup>2</sup> to 509.95 grams/m<sup>2</sup>. Plots 3, 4, and 5 exhibited grass biomass estimates that exceeded expected norms. Occupied volume on these plots varied from consistent with other plots having similar fuel loads to nearly twice the average volume of all plots. Surface area for

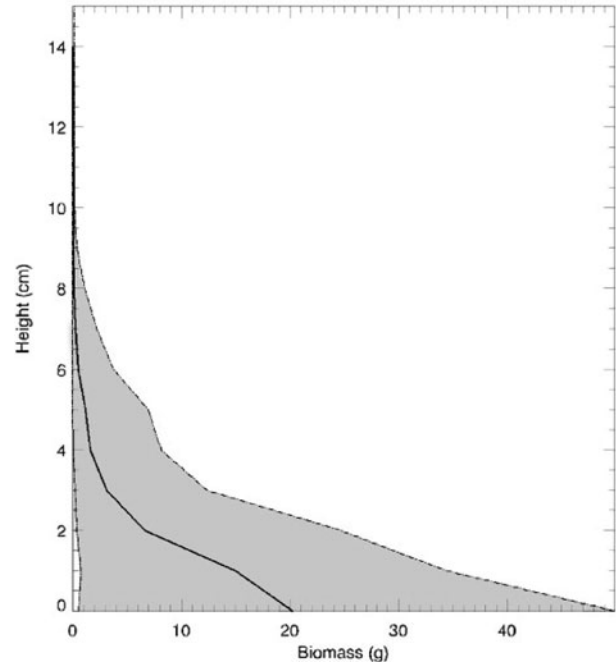


FIG. 4. Mean biomass for 1 cm height bins for all plots in Phase 1 are shown (solid line) bounded by standard deviation (dashed line). The bulk of biomass is allocated at the lowest strata of the fuelbed.

these same plots appears to be the primary driver of the larger biomass estimate because these plots average 150 % more surface area to volume than plots that fell within expected biomass ranges. Volume and surface area per plot for each fuel type are reported in Table 3. Estimates of longleaf pine needle litter biomass performed within published ranges. These fuel layers potentially produce the most realistic estimates of mass because the strata is limited in depth (between 2 cm–5 cm) and has very clear physical boundaries, whereas the grass fuels require more interpretation with regard to height and dispersion across the fuelbed. Bulk densities derived from the biomass and occupied volume averaged from 0.012 grams/cm<sup>3</sup> for grass to 0.077 grams/cm<sup>3</sup> for cones. Longleaf pine litter had an average bulk density of 0.0007 cm<sup>3</sup>.

Analysis of height distributions of biomass in the simulated fuelbeds shows that nearly 70 % of grass biomass is located below 5.5 cm height, which is where the height biomass curves inflect upward (Figure 4). This inflection height corresponds with the transition from grass bunch to the sparser stems and inflorescence. Additionally, about 40 % of the grass biomass occurs within 2 cm of the ground, occupying the litter layer more so than the aerial fuels within each fuel bed. All longleaf pine litter and deciduous oak litter biomass fell below the grass biomass inflection height described. Cone litter generally bisected the grass inflection height with fuel depth ranging from 5 cm to 8 cm.

TABLE 3  
 Occupied voxel volume (OV), surface area (SA), biomass (B), and bulk density (BD) is reported for grass, needle litter, and cones for each plot's subplot.

Plot	Subplot	Grass			Needle			Cone					
		OV (cm <sup>3</sup> )	SA (cm <sup>2</sup> )	B (g/m <sup>2</sup> )	BD (g/cm <sup>3</sup> )	OV (cm <sup>3</sup> )	SA (cm <sup>2</sup> )	B (g/m <sup>2</sup> )	BD (g/cm <sup>3</sup> )	OV (cm <sup>3</sup> )	SA (cm <sup>2</sup> )	B (g/m <sup>2</sup> )	BD (g/cm <sup>3</sup> )
1	1	11054	3663.21	56.78	0.005	17511	6932.18	16.09	0.0009	—	—	—	—
	2	11046	2801.95	43.43	0.004	18198	6487.15	15.05	0.0008	4697	63480.85	375.17	0.169
	3	21770	7263.36	112.58	0.005	18832	8735.35	20.27	0.0011	2285	28555.55	168.76	0.169
2	1	16684	4522.24	70.09	0.004	21933	15174.14	35.00	0.0016	4894	43556.27	257.42	0.169
	2	9360	2472.03	38.32	0.004	15174	10049.53	23.32	0.0015	—	—	—	—
	3	18439	5822.80	90.25	0.005	15174	15174.14	35.23	0.0023	6272	55960.62	330.73	0.189
3	1	51058	34956.00	541.82	0.011	4201	475.62	1.10	0.0003	4364	55138.75	325.87	0.133
	2	47682	38118.29	590.83	0.012	4729	505.45	1.17	0.0002	—	—	—	—
	3	24458	35151.61	544.85	0.022	12860	4376.90	10.16	0.0008	3290	40676.25	240.40	0.136
4	1	19909	19190.75	297.46	0.015	1015	92.87	0.22	0.0002	—	—	—	—
	2	22176	22199.45	344.09	0.016	1053	69.52	0.16	0.0002	4808	64623.56	381.93	0.125
	3	27793	38783.47	601.14	0.022	3863	238.07	0.55	0.0001	2382	33877.55	200.22	0.118
5	1	28619	42834.00	663.93	0.023	4465	319.45	0.74	0.0002	6169	86286.14	509.95	0.120
	2	28577	42853.20	664.22	0.023	8166	2131.55	4.95	0.0006	3105	43023.9	254.27	0.122
	3	30865	44981.79	697.22	0.023	3286	98.52	0.23	0.0001	—	—	—	—
6	1	10500	6805.63	105.49	0.010	9246	2546.17	5.91	0.0006	—	—	—	—
	2	11273	8774.84	136.01	0.012	2457	43.64	0.10	0.00004	1060	19959.0	117.96	0.898
	3	11208	8599.48	133.29	0.119	2457	43.64	0.10	0.00001	5299	73975.02	437.19	0.121
7	1	17074	234.19	3.63	0.0002	144	0.85	0.002	0.00001	—	—	—	—
	2	23257	7023.64	108.87	0.005	201	1.18	0.46	0.00001	2946	7887.48	174.1	0.169
	3	9209	2555.81	39.62	0.004	194	1.02	0.45	0.00001	4857	14382	287.04	0.169

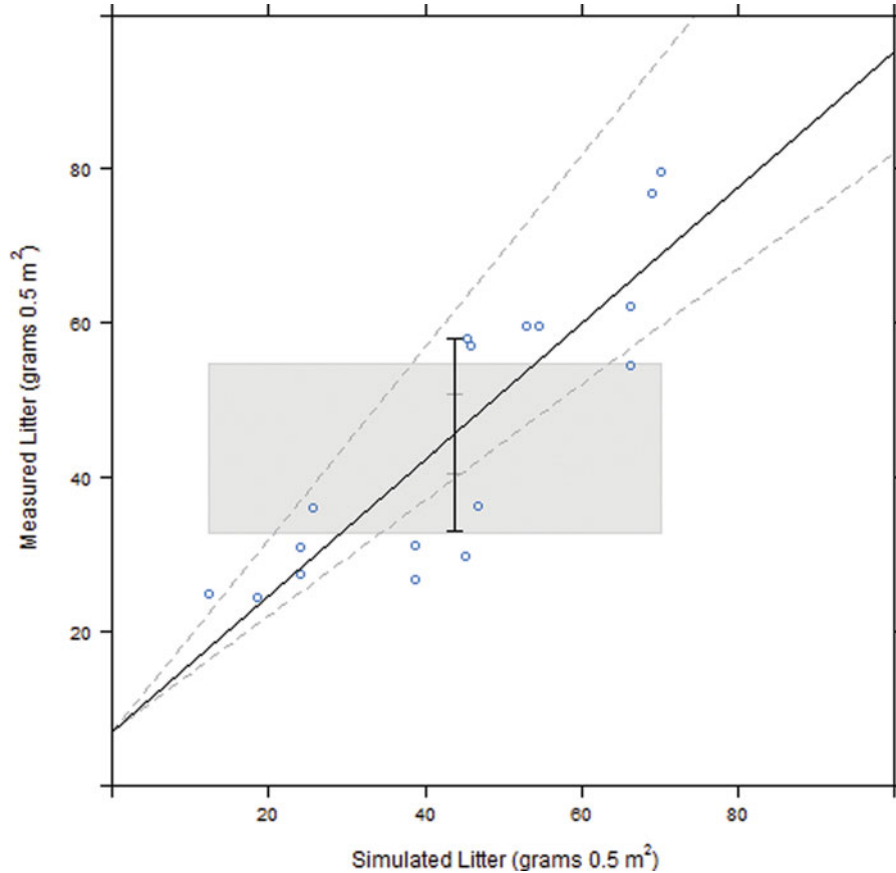


FIG. 5. An equivalence plot of the simulated litter and oven-dried litter biomass for each plot in the RxCadre validation.

### Phase 2: Validation and Comparison in the RxCadre Plots Biomass Validation

Biomass was estimated for the 3 dominant fuel types (needle litter, oak leaf litter, and perennial grasses) across the HIPs plots. The litter biomass estimates were combined into a single-litter value, because the weighed biomass is described in a single-litter term. Simulated litter biomass correlated well with oven-dried litter biomass ( $r = 0.86$ ,  $p < 0.05$ ,  $RMSE = 15.8$  g, Figure 5). Means were equivalent and ANOVA detailed no significant difference between mean simulated and actual litter biomass values ( $F = 1.05$ ,  $p < 0.93$ ,  $df = 16$ , confidence level = 0.95). Litter averaged 80 % ( $\sigma = 21$  %) of the total biomass for all clip plots combined from the weighed biomass data. Grass biomass represented a range of 2 % to 17 % of total biomass for 8 clip plots and simulated biomass again correlated well with oven-dried biomass; additionally, means were also equivalent ( $r = 0.98$ ,  $p < 0.05$ ,  $RMSE = 1.6$ g). Simulated forb biomass performed least well, though means were equivalent ( $r = 0.75$ ,  $p < 0.05$ ) revealing substantial variability in estimates when the species bracken fern models are present. There is difficulty in assessing if the error with these models is associated with the model or the field data classifications of emergent and nonemergent vegetation. In many of the plot photographs collected for

the experiment, bracken ferns are desiccated and in some cases have perched litter on top. Therefore, these ferns may also be partitioned to the litter fuel class.

### Phase 3: Weibull Distribution Comparison between Simulations and TLS

Weibull shape parameters ( $\alpha$ ) for the TLS-based point clouds and simulations compared well ( $r = 0.86$ ,  $p < 0.05$ , Figure 6) with equivalent means indicating that the Weibull slopes are similar in both datasets. Weibull  $\alpha$  parameters for the simulation data indicated a weak relationship with plots that are litter dominated ( $r = 0.65$ ,  $p < 0.05$ ), suggesting that low height objects in the litter bed influence the Weibull slope value. The scale parameters ( $\beta$ ) performed poorly ( $r = 0.21$ ,  $p < 0.5$ , Figure 7). The equivalence test demonstrated that the means were dissimilar. Clearly there are disparities in data density between the TLS and simulation data, with the simulation data density heavily weighted toward the litter bed ranging in height from 0 cm–5 cm. Several plots ( $n = 9$ ) were partially obscured by adjacent or overhanging vegetation, reducing the ability of the laser pulses to penetrate and accurately sample the litter layer of the plots (Figure 8).

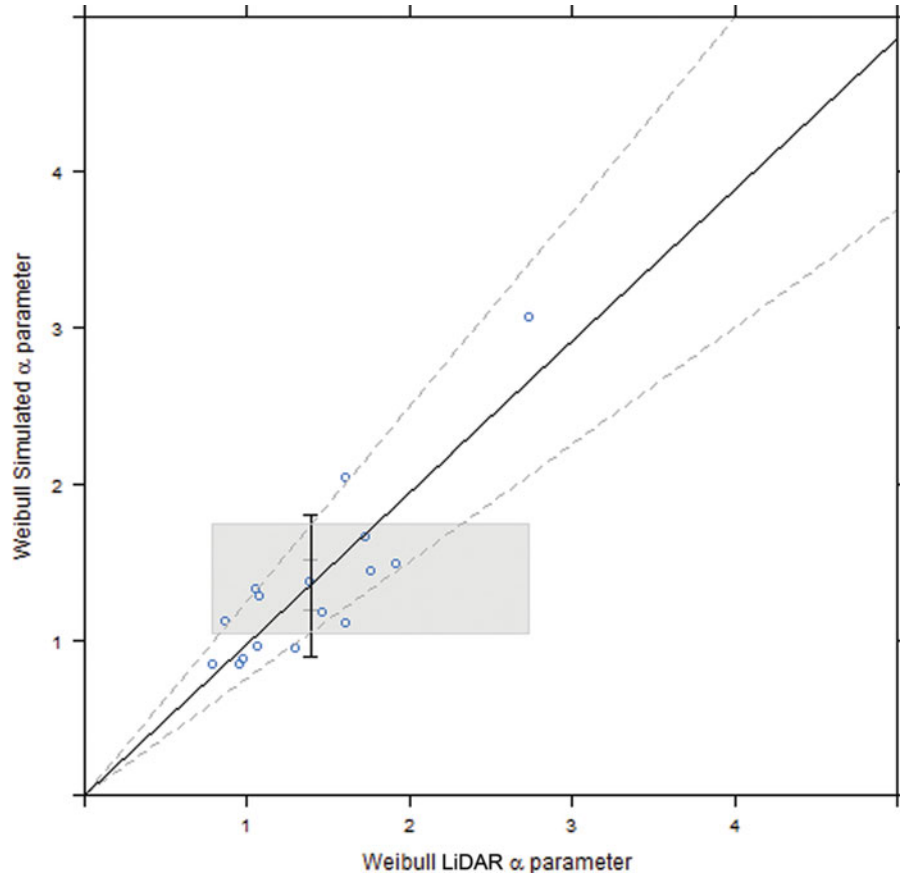


FIG. 6. An equivalence plot between the Weibull  $\alpha$  parameter derived from the TLS and simulation height distributions.

## DISCUSSION

This study provides a new approach for examining surface fuel variability at very fine scales (sub-m). Simulated fuelbeds produce a high degree of visual realism (Figure 2) and share height and biomass attributes with field measurements. These fuel models and their metrics can be used to design fuelbeds that are consistent in measurement of structure and biomass. This consistency in fuel attributes is currently missing from inputs needed for physics-based fire behavior models.

We view these fuelbed simulations as a bridge between field and remotely sensed data. Field sampling results in aggregation over large areas to infer average fuel loading (Ottmar et al. 2016). As discussed previously, traditional inventory methods simplify the fuelbed at the cost of characterizing the full range of variability that exists. Furthermore, an attempt to describe surface fuel mass, using airborne LiDAR, was inadequate in the same study area (Hudak et al. 2016). This may be attributable to the fine-scale heterogeneity of fuels associated with longleaf pine ecosystems, where there is a need to identify and spatially describe fuel distributions in regard to fuel type and fuel structure (Loudermilk et al. 2012; O'Brien et al. 2016).

We have demonstrated that these simulations are highly correlated to field-measured height and dry weight biomass. But

more importantly, these metrics can be allocated to specific fuel types, where other attempts using LiDAR have only looked at predicting overall fuel mass (Hudak et al. 2016) or predicting fuel models (Seielstad and Queen 2003). O'Brien et al. (2016) suggest the allocation to fuel type is a better predictor of subsequent fire radiative energy than fuel mass alone. Active remote sensing platforms, such as TLS, collect rich data, but assessing the individual fuel elements with differing properties within complex fuelbeds is difficult and has yet to be executed satisfactorily (Rowell and Seielstad 2012). In frequent low-intensity fire regimes, this specific allocation of fuel mass as a function of type and structure has the potential to quantify variability in fire radiative energy that contributes directly to fire effects (O'Brien et al. 2008; O'Brien et al. 2016).

The key difficulty with mapping surface fuels using TLS is uncertainty with regard to how the vertical distribution of the point cloud relates to complex matrices of fuels in the lowest strata of the fuelbed where the most influential fuels (e.g., pine litter, pinecones) are found. The simulation approach we describe in this study performs best for characterizing these particular fuel types. Previously, Coops et al. (2007) interpreted Weibull distributions of airborne LiDAR and related the Weibull  $\alpha$  and  $\beta$  parameters to characterize distributions of

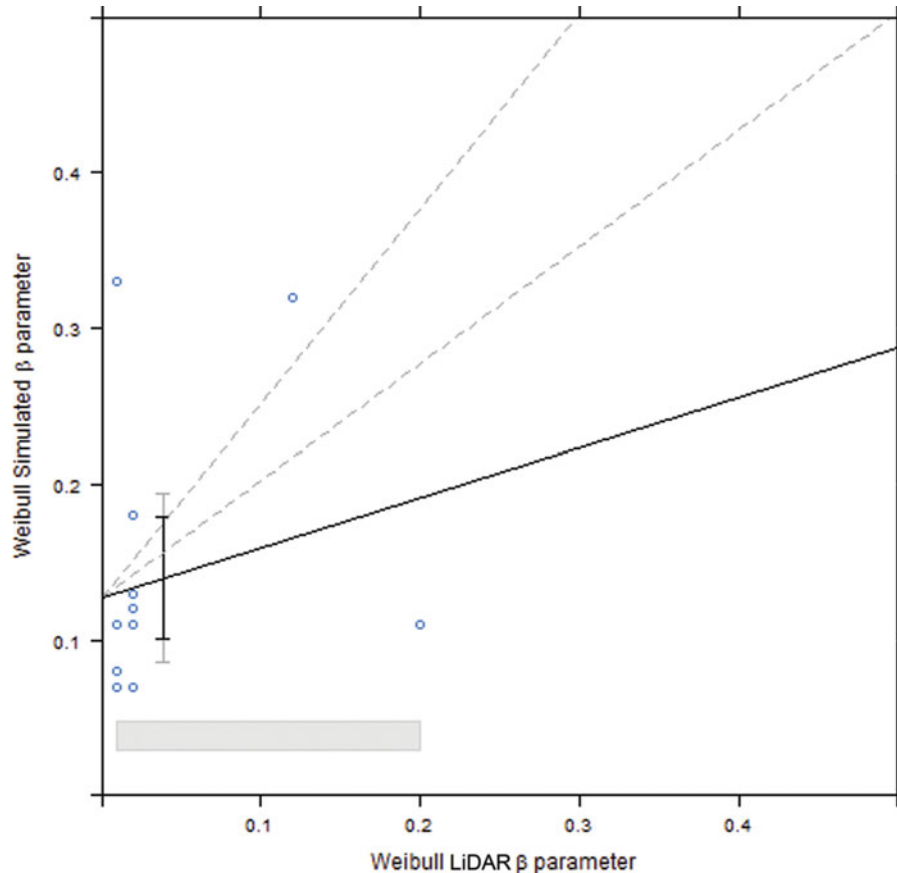


FIG. 7. An equivalence plot between the Weibull  $\beta$  parameter derived from the TLS and simulation height distributions.

biomass within forested canopies in British Columbia, Canada. This study found correlations between Weibull parameters of LiDAR canopy height models and field-measured height distributions, suggesting that airborne LiDAR data can be used to derive standard forest inventory information. For our research, it is clear that the amount of information we can glean from the surface fuels characterization of TLS-based height distributions is pivotal in characterizing fuel metrics. Within the RxCadre plots, TLS data underrepresent the bulk of fuels occurring at the lowest heights of the fuelbed. This requires inference from vertical distributions of the upper reaches of the fuelbed to predict what the configuration of the lowest height strata of grass and litter are. The Weibull  $\alpha$  parameters for both the TLS and simulated data suggest that we are describing the density of points and simulated objects distributed vertically.

The simulated Weibull distributions are based on the object vertices used to estimate surface area of the objects that are, in turn, used to predict biomass. From this, we infer that biomass is allocated similarly. Remington et al. (1992) demonstrated that the use of the 3-parameter Weibull characterizes grass biomass distributions based on grazing treatments in Colorado, USA. Our findings are similar to this study in that litter-dominated

plots are heavily weighted to lower heights with the highest concentrations of biomass.

Another important note is the effect of occlusion that results from laser pulses being intercepted by matter in the foreground or hanging over the plot of interest. Our analysis demonstrated that where this effect occurs, the ground surface sampling attenuates in regard to the actual number of objects present. Simulated fuelbeds capture these elements, and differences in the Weibull curves suggest that variability in TLS sampling might have a negative effect on predicting and distributing biomass in these systems. To overcome issues of occlusion, others have employed detailed and multiangle TLS acquisition to produce high-resolution scans that maximize laser pulse penetration into vegetation (Hosoi and Omasa 2009). Previous studies have demonstrated that for identifiable individual shrubs in large-area scans, TLS data can be used to estimate biomass across size gradients (Loudermilk et al. 2009; Olsoy et al. 2014; Greaves et al. 2015). The ability to discriminate specific intermixed fuel types and arrangements at the lowest reaches of the fuelbed is, therefore, difficult when utilizing TLS data.

We demonstrate that the simulated fuelbed approach produces meaningful estimates of leaf litter, grass, and forb biomass that are interspersed across the fuel matrix (Figure 8). These

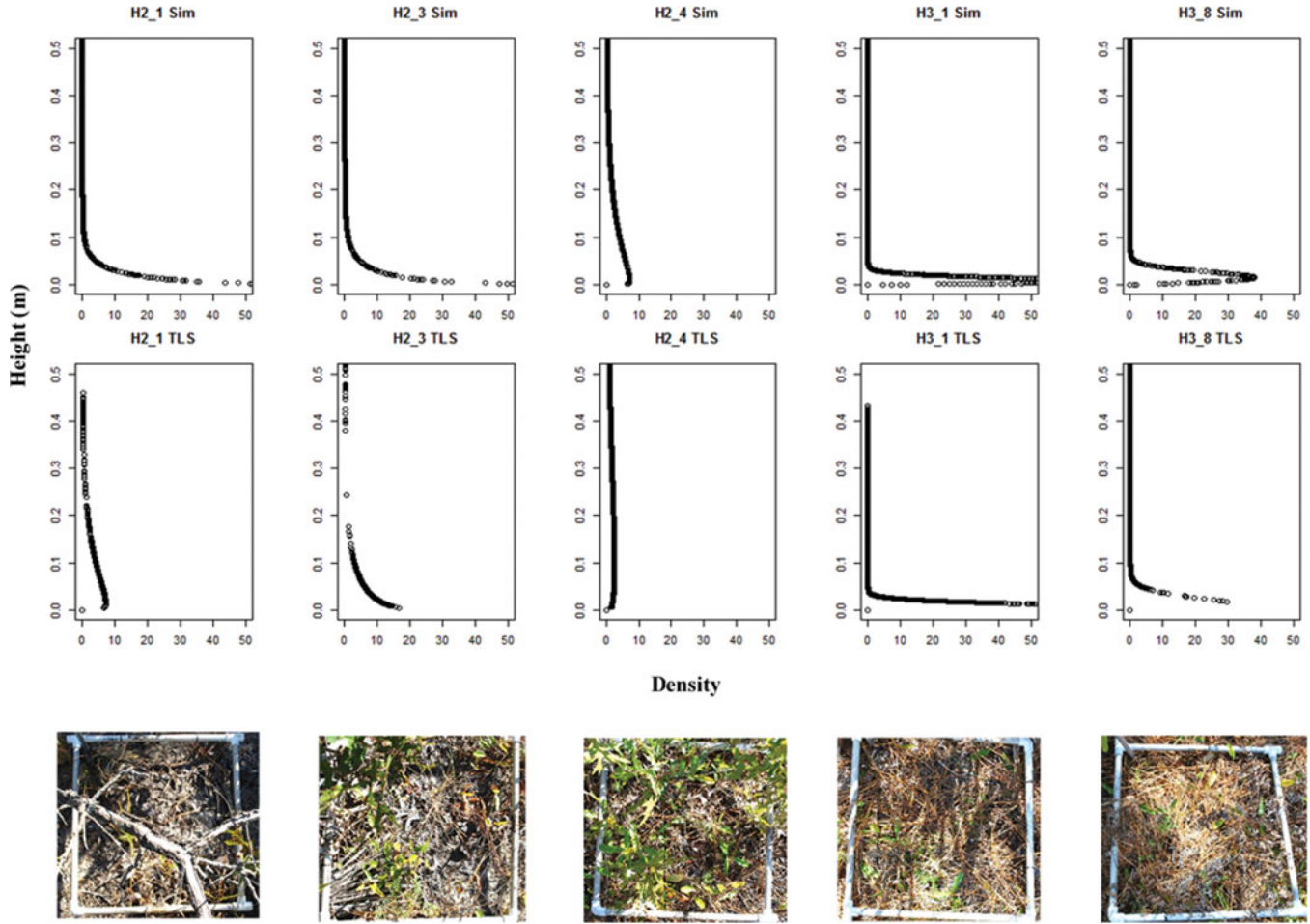


FIG. 8. Weibull distributions for 5 example plots used in the RxCadre experiment demonstrate similarities between simulations and TLS-based height profiles.

findings suggest that our simulations provide an enhanced range of variability by tying precise height and fuel load metrics with field-collected biomass. An advantage to this modeling technique is the absence of a priori knowledge of biomass to attribute across the fuelbed. Similarly, Parsons et al. (2011) attributes biomass to fractal tree models, using biomass estimates derived by the Forest Vegetation Simulator, where allometrically derived biomass is allocated across the tree-per-voxel unit as a function of branch and needle fuel type. Vertical and horizontal distributions of fuelbeds are critical in the realm of understanding the role of fuels in fire behavior and postcombustion fire effects. Our fuelbeds depicted higher concentrations of biomass (Figure 3) near the bottom of the fuelbed (<4 cm) in grass fuels and showed a higher degree of variability in the lower reaches of the fuelbed than higher up. Similarly, the ratio of occupied versus unoccupied space in the fuelbed changes with height, with more open space in the upper reaches of the fuelbed and less available biomass. We are also able to describe the horizontal distribution of fuels and decompose this distribution by fuel

type in a way that is not currently possible with field methods or remote sensing. An advantage to using this method is that estimates of biomass and bulk density are not prone to the same types of error that airborne or terrestrial LiDAR experience.

The description of fine-scale fuelbed biomass and partition is important because fuels differentially combust based on changes in relative humidity and ambient temperature. Varner et al. (2015) demonstrates the differences in combustion, specifically that longleaf pine needle litter has an intense, brief, and high-consumption burn period that makes this fuel type a primary carrier of fire in southeastern forests. Inversely, turkey oak litter has a long flaming and a protracted smoldering period. Being able to distinguish between important fuel types and respective mass is important for understanding factors that influence heat flux and postcombustion fire effects (O'Brien et al. in review). Andersen et al. (2004) describe small deviations from assumptions of uniform distributions of fuels that propagate significant effects of canopy bulk density in forested ecosystems. The ability to describe these fuels in terms of available biomass, volume,

and surface area by fuel type and across large areas is an exciting prospect for advancing wildland fire science.

### Future Work

We pose that limited field data does not need to inhibit finer-grain characterization of these fuelbeds. In fact, a combination of general height characteristics, photography, and fuel load might suffice to produce accurate simulated estimates of a variety of fuel arrangements encountered in a landscape. LiDAR data might act as a framework to distribute these simulated estimates of fuels through probability models or distribution analysis (Figure 6). However, characterizing large fuel beds (> 1 ha) using TLS is a difficult proposition. We suggest using Weibull relationships to link field data with TLS or airborne LiDAR vertical distributions with simulated fuelbeds as a way to populate a landscape. Specifically, integration of these data is crucial for creating consistent fuels data for validation of next-generation fire behavior models, such as the Wildland Fire Dynamic Simulator (WFDS; Mell et al. 2009) and FIRETEC/higrad (Linn et al. 2002). Although the resolutions of the simulated fuelbeds are computationally too expensive for integration into these fire behavior models, we suggest utilizing the TLS-based height distributions as a mechanism to extrapolate the amount and type of mass detailed in the simulations aggregated to coarser grain sizes. This technique could prove to be the most effective way to bridge the differences between field- and LiDAR-based measurements.

From the perspective of LiDAR remote sensing, having a dataset parameterized to represent realistic 3D distributions of fuels and biomass will serve as a backdrop for simulating laser point clouds via ray tracing. Disney et al. (2009) showed results that indicated the importance of LiDAR instrument settings and energy/matter interactions within simulated tree canopy structure, using the same parametric plant models as those in OnyxTree. This same study found that the ability to represent canopy architecture and elements discretely facilitated better understanding of how laser pulses penetrate tree crowns, with implications for predicting Leaf Area Index and related metrics (Disney et al. 2010). Palace et al. (2015) modeled canopy vegetation profiles and forest structure for comparison with similar airborne LiDAR metrics through simulated forest models in Costa Rican tropical forests. This study found that simulations that use established allometries to produce simulated forests found that canopy height is not a significant predictor of biomass, but modeling forest profiles that estimate plant area fractions improved LiDAR-derived estimates of forest biomass.

The ability to produce realistic simulated laser point clouds is a significant proving mechanism for understanding how TLSs characterize fine fuels. Previous attempts to describe these fuels have been difficult due to occlusion and point sampling variability using TLS data collected obliquely from a boom lift (Rowell et al. 2015). Further work needs to be conducted to determine how well biomass estimated from the simulated fu-

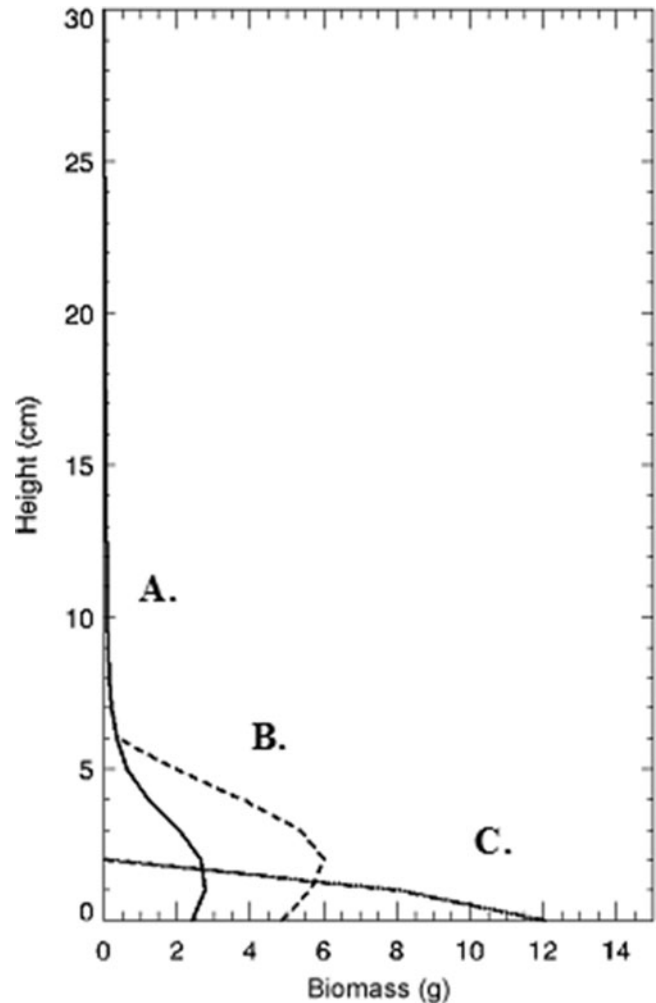


FIG. 9. Biomass distributions for a (A) mixed grass, (B) forb, and (C) litter plot demonstrating the vertical distribution of biomass per fuel type.

elbed performs, specifically integrating more intensely sampled fuelbeds. Automation of fuelbed construction is also imperative to reducing variability and subjectivity. We also foresee benefits for the integration of these findings with other high-resolution simulation techniques, such as FUEL3D (Parsons 2006), with which we may begin to combine surface and canopy fuels for improved inputs used for physics-based fire behavior models.

### CONCLUSIONS

In this article, we presented results that demonstrate 3D fuelbed simulations can explain much of the variability of biomass allocation and height distributions that are difficult to estimate using TLS data. Although the approach to building these simulations needs improvement in terms of automation and further validation, there is significant promise for using these methods to populate spatial datasets for use in complex-fluid-dynamics-based fire behavior models. Assumptions of plant structure,

biomass partition, and height estimation need to be refined to include a broader diversity of species found in the southeastern United States and similarly structured ecosystems worldwide. We intend to further investigate the integration of these surface fuelbed simulations with other canopy fuel modeling techniques (e.g., FUEL3D) and the ability to leverage remotely sensed data to extrapolate landscape-scale fuelbed models.

## ACKNOWLEDGMENTS

The authors wish to thank Jackson Guard Wildland Fire personnel at Eglin Air Force Base, Florida, for their professionalism and continuous support, specifically Brett Williams of the Air Force Wildland Fire Center, Scott Pokswinski, University of Nevada, Reno, the Forestry Sciences Laboratory of the Southern Research Station, Athens, GA, and staff of the National Center for Landscape Fire Analysis with TLS data collection. Special thanks go to Mat Disney, University College London, for the inspiration of the fuelbed simulations.

## FUNDING

This study was funded in part by the DoD Strategic Environmental Research and Development Program grant RC-2243, Joint Fire Science Programs (11-2-1-11), and the National Center for Landscape Fire Analysis.

## REFERENCES

- Andersen, H.E., McGaughey, R.J., and Reutebuch, S.E. 2004. "Estimating forest canopy fuel parameters using LIDAR data." *Remote Sensing of Environment*, Vol. 94: pp. 441–449. doi:10.1016/j.rse.2004.10.013.
- Brockway, D.G., and Outcalt, K.W. 2000. "Restoring longleaf pine wiregrass ecosystems: hexazinone application enhances effects of prescribed fire." *Forest Ecology and Management*, Vol. 137: pp. 121–138.
- Brown, J.K. 1974. *Handbook for Inventorying Downed Woody Material*. General Technical Report INT-16, Intermountain Forest & Range Experiment Station, Odgen, UT: USDA Forest Service.
- Brown, J.K. 1981. "Bulk densities of non uniform surface fuels and their application to fire modeling." *Forest Science*, Vol. 27(No. 4): pp. 667–683.
- Cawse-Nicholson, K., van Aardt, J., Romanczyk, P., Kelbe, D., Krause, K., and Kampe, T. 2013. "A study of energy attenuation due to forest canopy in small-footprint waveform LiDAR signals." In *Proceedings of the American Society for Photogrammetry and Remote Sensing (ASPRS)*, Baltimore, MD, USA.
- Coops, N.C., Hilker, T., Wulder, M.A., St-Onge, B., Newham, G., Siggins, A., and Trofymow, J.A. 2007. "Estimating canopy structure of Douglas-fir forest stands from discrete-return LiDAR." *Trees*, Vol. 21: pp. 295–310. doi: 10.1007/s00468-006-0119-6.
- Delignette-Muller, M.L. and Dutang, C. 2015. "fitdistrplus: An R Package for Fitting Distributions." *Journal of Statistical Software*, Vol. 64(No. 4): pp. 1–34. <http://www.jstatsoft.org/v64/i04/>
- Derner, J.D., Briske, D.D., and Polley, H.W. 2012. "Tiller organization within the tussock grass *Schizachyrium scoparium*: A field assessment of competition-cooperation tradeoffs." *Botany*, Vol. 90: pp. 669–677.
- Disney, M.I., Kalogirou, V., Lewis, P., Prieto-Blanco, A., Hancock, S., and Pfeifer, M. 2010. "Simulating the impact of discrete-return LiDAR system and survey characteristics over young conifer and broadleaf forests." *Remote Sensing of Environment*, Vol. 114: pp. 1546–1560. doi:10.1016/j.rse.2010.02.009.
- Disney, M.I., Lewis, P.E., Bouvet, M., Prieto-Blanco, A., and Hancock, S. 2009. "Quantifying surface reflectivity for spaceborne LiDAR via two independent methods." *IEEE Transactions on Geoscience and Remote Sensing*, Vol. 47(No. 9): pp. 3262–3271.
- Disney, M.I., Lewis, P., Gomez-Dans, J., Roy, D., Wooster, M.J., and Lajas, D. 2011. "3D radiative transfer modelling of fire impacts on a two-layer savanna system." *Remote Sensing of Environment*, Vol. 115: pp. 1866–1881. doi:10.1016/j.rse.2011.03.010.
- Fonda, R.W. 2001. "Burning characteristics of needles from eight pine species." *Forest Science*, Vol. 47: pp. 390–396.
- Fonda, R., and Varner, J.M. 2004. Burning characteristics of cones from eight pine species. *Northwest Science*, Vol. 78: pp. 322–333.
- Greaves, H.E., Vierling, L.A., Eitel, J., Boelman, N.T., Magney, T.S., Prager, C.M., Griffin, K.L. 2015. "Estimating aboveground biomass and leaf area of low-stature Arctic shrubs with terrestrial LiDAR." *Remote Sensing of Environment* Vol. 164: pp. 26–35. doi:10.1016/j.rse.2015.02.023.
- Glenn, N.F., Spaete, L.P., Sankey, T.T., Derryberry, D.R., Hardegree, S.P., and Mitchell, J.J. 2010. "Errors in LiDAR-derived shrub height and crown area on sloped terrain." *Journal of Arid Environments* Vol. 75: pp. 377–382. doi: 10.1016/j.jaridenv.2010.11.005.
- Hardy, C., Heilman, W., Weise, D., Goodrick, S., and Ottmar, R. 2008. "Fire behavior advancement plan; a plan for addressing physical fire processes within the core fire science portfolio." Final report to the Joint Fire Sciences Program Board of Governors, accessed March 10, 2012, [http://www.fire-science.gov/projects/08-S-01/project/08-S-01\\_final\\_report\\_08-s-01.pdf](http://www.fire-science.gov/projects/08-S-01/project/08-S-01_final_report_08-s-01.pdf)
- Hiers, J.K., O'Brien, J.J., Mitchell, R.J., Grego, J.M., and Loudermilk, E.L. 2009. "The wildland fuel cell concept: an approach to characterize fine-scale variation in fuels and fire in frequently burned longleaf pine forests." *International Journal of Wildland Fire* Vol. 18: pp. 315–325. doi: 10.1071/WF08084.
- Hopkinson, C., Chasmer, L.E., Sass, G., Creed, I.F., Sitar, M., Kalbfleisch, W., and Treitz, P. 2005. "Vegetation class dependent errors in LiDAR ground elevation and canopy height estimates in a boreal wetland environment." *Canadian Journal of Remote Sensing*, Vol. 31(No. 2): pp. 191–206.
- Hosoi, F., and Omasa, K. 2006. "Voxel-based 3-D modeling of individual trees for estimating leaf area density using high-resolution portable scanning LiDAR." *IEEE Transactions on Geoscience and Remote Sensing* Vol. 44: pp. 3610–3618. doi: 10.1109/TGRS.2006.881743.
- Hudak, A.T., Dickinson, M.B., Bright, B.C., Kremens, R.L., Loudermilk, E.L., O'Brien, J.J., Hornsby, B.S., and Ottmar, R.D. 2016. "Measurements related to fire radiative energy density and surface fuel consumption – RxCADRE 2011 and 2012." *International Journal of Wildland Fire*, Vol. 25: pp. 25–37. doi: 10.1071/WF14159.
- Kane, J.M., Varner, J.M., and Hiers, J. 2008. "The burning characteristics of southeastern oaks: Discriminating fire facilitators from fire impeters." *Forest Ecology and Management*, Vol. 256(No. 12): pp. 2039–2045. doi:10.1016/j.foreco.2008.07.039.
- Keane, R.E., Burgan, R., and van Wagtenonk, J. 2001. "Mapping wildland fuels for fire management across multiple scales: integrating re-

- mote sensing, GIS, and biophysical modeling." *International Journal of Wildland Fire*, Vol. 10: pp. 301–319. doi: 10.1071/WF01028.
- Linn, R.R., Reisner, J., Colman, J., and Winterkamp, J. 2002. "Studying wildfire using FIRETEC." *International Journal of Wildland Fire* Vol. 11: pp. 1–14.
- Loudermilk, E.L., Hiers, J.K., O'Brien, J.J., Mitchell, R.J., Singhania, A., Fernandez, J.C., Cropper, W.P., and Slatton, K.C. 2009. "Ground-based LIDAR: a novel approach to quantify fine-scale fuelbed characteristics." *International Journal of Wildland Fire*, Vol. 18: pp. 676–685. doi: 10.1071/WF07138.
- Loudermilk, E.L., O'Brien, J.J., Mitchell, R.J., Cropper, W.P., Hiers, J.K., Grunwald, S., Grego, J., and Fernandez-Diaz, J.C. 2012. "Linking complex forest fuel structure and fire behaviour at fine scales." *International Journal of Wildland Fire*, Vol. 21: pp. 882–893. doi: 10.1071/WF10116.
- Loudermilk, E.L., Stanton, A., Scheller, R.M., Dilts, T.E., Weisberg, P.J., Skinner, C., and Yang, J. 2014. "Effectiveness of fuel treatments for mitigating wildfire risk and sequestering forest carbon: a case study in the Lake Tahoe Basin." *Forest Ecology and Management*, Vol. 323 (No. 1): pp. 114–125. doi: 10.1016/j.foreco.2014.03.011.
- Mell, W., Maranghides, A., McDermott, R., and Manzello, S.L. 2009. "Numerical simulation and experiments of burning Douglas fir trees." *Combustion and Flame*. Vol. 156: pp. 2023–2041
- Mitchell, R.J., Hiers, J.K., O'Brien, J., and Starr, G. 2009. "Ecological forestry in the Southeast understanding the ecology of fuels." *Journal of Forestry*, Vol. 107 (No. 8): pp. 391–397.
- Mutch, R.W., Arno, S.F., Brown, J.K., Carlson, C.E., Ottmar, R.D., and Peterson, J.L. 1993. *Forest Health in the Blue Mountains: A Management Strategy for Fire-Adapted Ecosystems*. General Technical Report PNW-GTR-310. Portland, OR: USDA Forest Service.
- O'Brien, J.J., Hiers, J.K., Callahan, M.A., Mitchell, R.J., and Jack, S. 2008. "Interactions among overstory structure, seedling life-history traits and fire in frequently burned neotropical pine forests." *Ambio* Vol. 37: pp. 542–547.
- O'Brien, J.J., Loudermilk, E.L., Hornsby, B., Hudak, A.T., Bright, B.C., Dickinson, M.B., Hiers, J.K., Teske, C., and Ottmar, R.D. 2016. "High-resolution infrared thermography for capturing wildland fire behavior – RxCADRE 2012." *International Journal of Wildland Fire*, Vol. 25: pp. 62–75. doi: 10.1071/WF14165.
- O'Brien, J.J., Loudermilk, E.L., Hornsby, B., Polswinski, S., Hudak, A., Strother, Rowell, E., Bright, B. 2016. Canopy derived fuels drive patterns of in-fire energy release and understory plant mortality in a longleaf pine *Pinus palustris* sandhill in Northwest Florida, USA. *Canadian Journal of Remote Sensing* doi: 10.1080/07038992.2016.1199271.
- Olsoy, P., Glenn, N., Clark, P., and Derryberry, D. 2014. "Aboveground total and green biomass of dryland shrub derived from terrestrial laser scanning." *ISPRS Journal of Photogrammetry and Remote Sensing*, Vol. 88: pp. 166–173. doi: 10.1016/j.isprsjprs.2013.12.006.
- Ottmar, R.D., Hudak A.T., Prichard, S.J., Wright, C.S., Restaino, J.C., Kennedy, M.C., and Vihnanek, R.E. 2016. "Pre-fire and post-fire surface fuel and cover measurements collected in the southeastern United States for model evaluation and development—RxCADRE 2008, 2011, and 2012". *International Journal of Wildland Fire*, Vol. 25: pp. 10–24. doi: 10.1071/WF15092
- Palace, M.W., Sullivan, F.B., Ducey, M.J., Treuhaft, R.N., Herrick, C., Shimbo, J.Z., and Mota-E-Silva, J. 2015. "Estimating forest structure in a tropical forest using field measurements, a synthetic model and discrete return LiDAR data." *Remote Sensing of Environment*, Vol. 161: pp. 1–11. doi: 10.1016/j.rse.2015.01.020.
- Parsons, R. 2006. "FUEL-3D: A spatially explicit fractal fuel distribution model." In *Fuels Management—How to Measure Success: Conference Proceedings*. Proceedings RMRS-P-41, Rocky Mountain Research Station. Fort Collins, CO: USDA Forest Service.
- Parsons, R.A., Mell, W.E., and McCauley, P. 2011. "Linking 3D spatial models of fuels and fire: effect of spatial heterogeneity on fire behavior." *Ecological Modelling*, Vol. 222: pp. 679–691.
- Popescu, S.C., Wynne, R.H., and Nelson, R.F. 2002. "Estimating plot-level tree heights with LiDAR: local filtering with a canopy-height based variable window size." *Computers and Electronics in Agriculture* Vol. 37(No. 1): pp. 71–95. doi: 10.1016/S0168-169902.00121-7.
- Prince, D.R., Fletcher, M.E., Shen, C., and Fletcher, T.H. 2014. "Application of L-systems to geometrical construction of chamise and juniper shrubs." *Ecological Modelling*, Vol. 273: pp. 86–95. doi: 10.1016/j.ecolmodel.2013.11.001.
- Prince, D.R. 2014. *Measurement and Modeling of Fire Behavior in Leaves and Sparse Shrubs*. Dissertation, Brigham Young University, Provo, Utah, USA.
- Remington, K.K., Bonham, C.D., and Reich, R.M. 1992. "Blue grama-buffalograss responds to grazing: a Weibull distribution." *Journal of Range Management*, Vol. 45: pp. 272–276.
- Riaño, D., Chuvieco, E., Ustin, S.L., Salas, J., Rodriguez-Pérez, J.R., Ribeiro, L.M., and Viegas, D.X. 2007. "Estimation of shrub height for fuel type mapping combining airborne LiDAR and simultaneous color infrared ortho imaging." *International Journal of Wildland Fire*, Vol. 16(No. 3): pp. 341–348. doi: 10.1071/WF06003.
- Robinson, A. 2016. *Equivalence R Package*, Version 0.7.2. <https://cran.r-project.org/web/packages/equivalence/index.html>
- Robinson, A.P., Duursma, R.A., and Marshall, J.D. 2005. "A regression-based equivalence test for model validation: shifting the burden of proof." *Tree Physiology*, Vol. 25: pp. 903–913.
- Rowell, E., and Seielstad, C. 2012. "Characterizing grass, litter, and shrub fuels in longleaf pine forest pre-and post-fire using terrestrial LiDAR." *SilviLaser 2012*, pp. 1–8, Vancouver, Canada, September 16–19, 2012.
- Rowell, E.M., Seielstad, C.A., and Ottmar, R.D. 2015. "Developing and validating fuel height models for the RxCADRE experiments." *International Journal of Wildland Fire*, Vol. 25: pp. 38–47. doi: 10.1071/WF14170.
- Sandberg, D.V., Hardy, C.C., Weise, D.R., Rehm, R., and Linn, R.R. 2003. "Core fire science caucus." Second International Wildland Fire Ecology and Fire Management Congress. Association for Fire Ecology, Orlando, FL, November 16–20, 2003.
- Seielstad, C.A., and Queen, L.P. 2003. "Using airborne laser altimetry to determine fuel models for estimating fire behavior." *Journal of Forestry*. Vol. 101(No. 4): pp. 10–15
- Stoker, J. 2009. "Volumetric visualization of multiple return LIDAR data – using voxels." *Photogrammetric Engineering and Remote Sensing*, Vol. 75(No. 2): pp. 109–112.
- Strecker, D., and Glenn, N. 2006. "LiDAR measurements of sagebrush steppe vegetation heights." *Remote Sensing of Environment*, Vol. 102(No. 1): pp. 135–145. doi: 10.1016/j.rse.2006.02.011.

- Thaxton, J.M., and Platt, W.J. 2006. "Small-scale variation alters fire intensity and shrub abundance in a pine savanna." *Ecology*, Vol. 87(No. 5): pp. 1331–1337.
- Thompson, W.L. 2004. *Sampling Rare or Elusive Species: Concepts, Designs, and Techniques for Estimating Population Parameters*. Washington, DC: Island Press.
- Van Wagner, C.E. 1968. "The line intersect method in forest fuel sampling." *Forest Science*, Vol. 14(No. 1): pp. 20–27.
- Varner, J.M., Kane, J.M., Banwell, E.M., and Krye, J.K. 2015. "Flammability of litter from southeastern trees: A preliminary assessment." In *Proceedings of the 17th Biennial Southern Silvicultural Research Conference*, General Technical Report SRS–203, Southern Research Station. Asheville, NC: USDA Forest Service.
- Vierling, L., Xu, Y., Eitel, J., and Oldow, J. 2013. Shrub characterization using terrestrial laser scanning and implications for airborne LiDAR assessment. *Canadian Journal of Remote Sensing* Vol. 38(No. 6): pp. 709–722. doi: 10.5589/m12-057.
- Woodgate, W., Disney, M., Armston, J.D., Jones, S.D., Suarez, L., Hill, M.J., Wilkes, P., Soto-Berelev, M., Haywood, A., and Mellor, A. 2015. "An improved theoretical model of canopy gap probability for Leaf Area Index estimation in woody ecosystems." *Forest Ecology and Management*, Vol. 358 (No. 15): pp. 303–320. doi: 10.1016/j.foreco.2015.09.030.